CHAPTER 2

Dust origins in the Milky Way

The recent availability of high quality observational data for diffuse regions in the Milky Way (MW) and external galaxies have added to our understanding of interstellar dust. A comparison of ultraviolet (UV) and infrared (IR) observations may be used to estimate absorption, scattering and thermal re-emission caused by the dust grains. In this chapter, we have looked for infrared counterparts of diffuse far-ultraviolet (FUV) sources in the Galaxy using observations from space-based telescope archives. The data presented here is unique and our study tries to find the origins of various dust populations at low and high latitude locations in the Galaxy by studying the FUV-IR correlation trends.

2.1 Motivation

As discussed in Chapter 1, in spite of the existence of multiple dust models, the most accepted view is that interstellar dust grains consist of amorphous silicates and some form of carbonaceous materials. In the mid-infrared (MIR), we observe emission from small Polycyclic Aromatic Hydrocarbon (PAH) molecules [103] and solid grains which have sizes starting from a few tens of Å [1]. These solid grains are known as Very Small Grains (VSGs) and their emission is detected around 24 μm [104, 105]. PAH molecules are electronically excited by the background UV photons and they emit in the MIR through infrared fluorescence with a significant amount of emission observed near 8 μm [23, 105]. The (8 μm /24 μm) surface brightness ratio is observed to be high in the diffuse ISM and low in bright star-forming regions [105]. There have been large scale observations of diffuse dust emission in the Galaxy with the advent of space-based telescopes such as the *Spitzer Space Telescope*, *Far Ultraviolet Spectroscopic Explorer (FUSE)* and *Galaxy Evolution Explorer (GALEX)*. Earlier studies [106] have not found any correlation among the diffuse FUV and cold dust emission around 100 μm in the Galaxy. Hence, by studying the FUV-IR correlations separately for low and high latitude locations, we hope to probe the dust properties in the MW and give accurate explanations for the observed correlation trends.

2.2 Sample of Observations

The sample of diffuse dust locations showing FUV scattering in the Galaxy has been selected from observations made by three UV space telescopes: *Voyager* [107–109], *FUSE* [109, 110] and *GALEX* [75]. The related instruments and data reduction techniques have been well documented in the individual sources [75, 107–110] which have provided the diffuse dust locations and corresponding FUV observations for this work.

The *Voyager UVS*, with a large field of view of $0.1°\times0.87°$, observed diffuse radiation from 500-1600 Å with a resolution of about 38 Å. It had long integration times resulting in a high sensitivity to diffuse radiation, i.e. better than 100 photons cm^{-2} sr^{-1} s^{-1} $Å^{-1}$ [109]. The *FUSE* telescope had the *LWRS* ($30''\times30''$) aperture on-board and the four *FUSE* spectrographs with a resolution ($\lambda/\Delta\lambda$) of about 20000 covered the 850-1167 Å wavelength range. It could detect background levels of 2000 photons cm^{-2} sr^{-1} s^{-1} $Å^{-1}$ [109]. Murthy & Sahnow (2004) [110] have described in details the method of extracting the diffuse surface brightness from FUSE observations. It involved collapsing the spectra into two wavelength bands per detector by treating the FUSE spectrum as a broadband photometric observation and excluding the terrestrial air glow lines (primarily Lyβ). The *GALEX* telescope details have been discussed in Section 1.2.1.

Our locations include the Coalsack nebula, which is one of the prominent dark nebulae in the southern sky of the Milky Way. The emission from the nebula is mainly due to the forward scattering of light from the bright stars behind it [107]. While Infrared Spectrograph (IRS) from *Spitzer* provides the most accurate way to study the dust features, it would be beneficial to use some combination of Infrared Array Camera (IRAC) [76] and Multiband Imaging Photometer for Spitzer (MIPS) [77] images since having a photometric probe would allow for a larger range of objects and environments to be studied given that imaging is faster to acquire and can probe regions that are too faint for spectroscopy. The 8 μm band of IRAC is designed to cover the 7.7 μm PAH feature, while the 24 μm of MIPS just covers the dust continuum from VSGs for local galaxies, avoiding the contamination of most of the MIR emission or absorption lines. The IRAC and MIPS instrument details have been discussed in Section 1.2.1. We found archival data for 48 dust locations observed at 8 μm by IRAC and 80 dust locations observed at 24 μm by MIPS in the Spitzer Heritage Archive (SHA). Figure 2.1 shows our dust locations plotted on an all-sky map of the FUV diffuse sky [75].

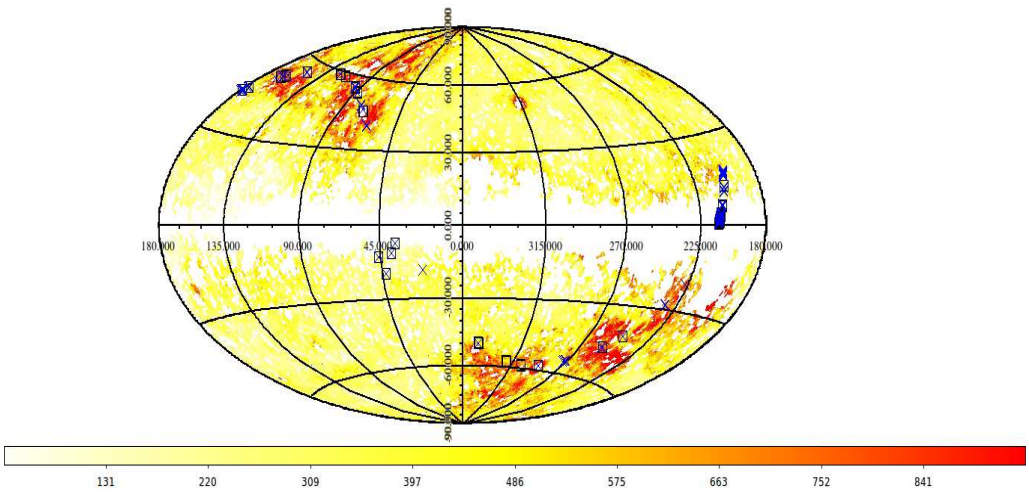

Figure 2.1: Our locations plotted on an Aitoff with Galactic coordinates. The 8 μm locations are represented as blue squares and 24 μm locations as blue crosses. This is an all-sky map of the FUV diffuse sky [75].

2.3 Data analysis and Results

We have calculated the emission intensities at the 48 diffuse dust locations with 8 μm data and the 80 locations with 24 μm data using aperture photometry as discussed in Section 1.3.1. We have used *Spitzer* post basic calibrated data (pbcd) and treated the images at different wavelengths independently. After computing the IR intensities, we have calculated the Spearman's rank correlation coefficient (ρ) as discussed in Section 1.3.2. We have calculated the rank correlations between the intensity values for the FUV data and the MIR data at the same dust locations.

As the source of FUV radiation could be different at low and high latitudes locations with dust grains being the main contributor at moderate to low latitudes, we have separated our data into high and low Galactic latitude locations and calculated the correlations separately. Locations within the range $-20^\circ \leq |b| \leq 20^\circ$ are considered to be low latitude and those in the range $|b| > 20^\circ$ to $|b| < -20^\circ$ are considered to be high latitude, 'b' being the Galactic latitude. We have also included the correlations between the hydrogen column density, N(H) and the MIR intensities. In order to calculate the value of N(H), we have used the all-sky 100 μm dust emission map by Schlegel et al. (1998) [111] to extract the color excess, E(B-V) for our locations. We have then used the following relation for total to selective extinction at the B and V filter bands in order to obtain the total extinction A(V) for each location:

$$\frac{A(V)}{E(B-V)} = R(V) \tag{2.1}$$

where R(V) = 3.1 for the Milky Way [1]. The value of A(V) is then substituted in the following:

$$\frac{N(H)}{A(V)} = 1.8 \times 10^{21} \ atoms\, cm^{-2}\, mag^{-1} \tag{2.2}$$

to obtain the required value of N(H) for that particular location.

The optical depth is given by $\tau(\lambda) = N(H) \times \sigma$, where $\lambda = 1500$ Å and σ is the extinction cross-section. Here, as the number density of particles increases, the scattering also increases ($n\sigma$). Now, if σ goes higher, there will be multiple scattering that dominates, much before τ approaches 1 since the albedo will be higher. At high values of σ and resultant τ, we will have significantly high extinction ($e^{-\tau}$). But multiple scattering will dominate at low latitudes and lead to more absorption. Hence, the scattered intensities are no longer linear with n, i.e. τ and this will heavily affect the correlation values. It will be linear only in case of single scattering. At low values, $\tau \ll 1$, single scattering dominates. For the lower latitude locations with a cutoff value of $N(H) = 9 \times 10^{21}$ cm^{-2}, we have $\tau = 0.0916$, while for the higher latitude locations with a cutoff value of $N(H) = 3 \times 10^{20}$ cm^{-2}, we have $\tau = 0.00305$ which correspond to the values of σ at $\lambda = 1500$ Å [1]. Hence, we use a cutoff (k) on N(H) to keep multiple scattering in check by keeping τ low such that it does not affect our observed correlations.

We have 48 locations with FUV and corresponding 8 μm data. Among these, 22 are low latitude locations while 26 are high latitude locations. Similarly, we have 80 locations with 24 μm data among which 39 are low latitude locations while 41 are high latitude locations. We have calculated the Spearman's rank correlations with and without a cutoff (k) on the value of N(H). The low latitude correlations are listed in Table 2.1 and the plots are shown in Figures 2.2 and 2.3. The axes labeled as 'I' with a subscript indicate the intensity at that particular wavelength, e.g. $I_{8\mu m}$ indicates intensity at 8 μm. The high latitude correlations are listed in Table 2.2 and shown in Figures 2.4 and 2.5.

Table 2.1: Rank correlation coefficients (ρ) for the 22 low latitude locations having 8 μm data and 39 low latitude locations having 24 μm data. Here, k means a cutoff for N(H) at 9×10^{21} cm^{-2}.

Wavelength	ρ	p-value
8 μm vs. N(H)	0.852	4.776e-07
8 μm vs. N(H)(k)	0.900	0.0374
8 μm vs. FUV	-0.072	0.751
8 μm vs. FUV(k)	0.500	0.391
24 μm vs. N(H)	0.742	6.617e-08
24 μm vs. N(H)(k)	0.183	0.454
24 μm vs. FUV	-0.008	0.963
24 μm vs. FUV(k)	-0.602	0.006

Table 2.2: Rank correlation coefficients (ρ) for the 28 high latitude locations having 8 μm data and 41 high latitude locations having 24 μm data. Here, k means a cutoff for N(H) at 3×10^{20} cm^{-2}.

Wavelength	ρ	p-value
8 μm vs. N(H)	0.343	0.086
8 μm vs. N(H)(k)	0.469	0.021
8 μm vs. FUV	0.296	0.141
8 μm vs. FUV(k)	0.356	0.087
24 μm vs. N(H)	-0.019	0.906
24 μm vs. N(H)(k)	0.217	0.224
24 μm vs. FUV	0.165	0.301
24 μm vs. FUV(k)	0.218	0.223

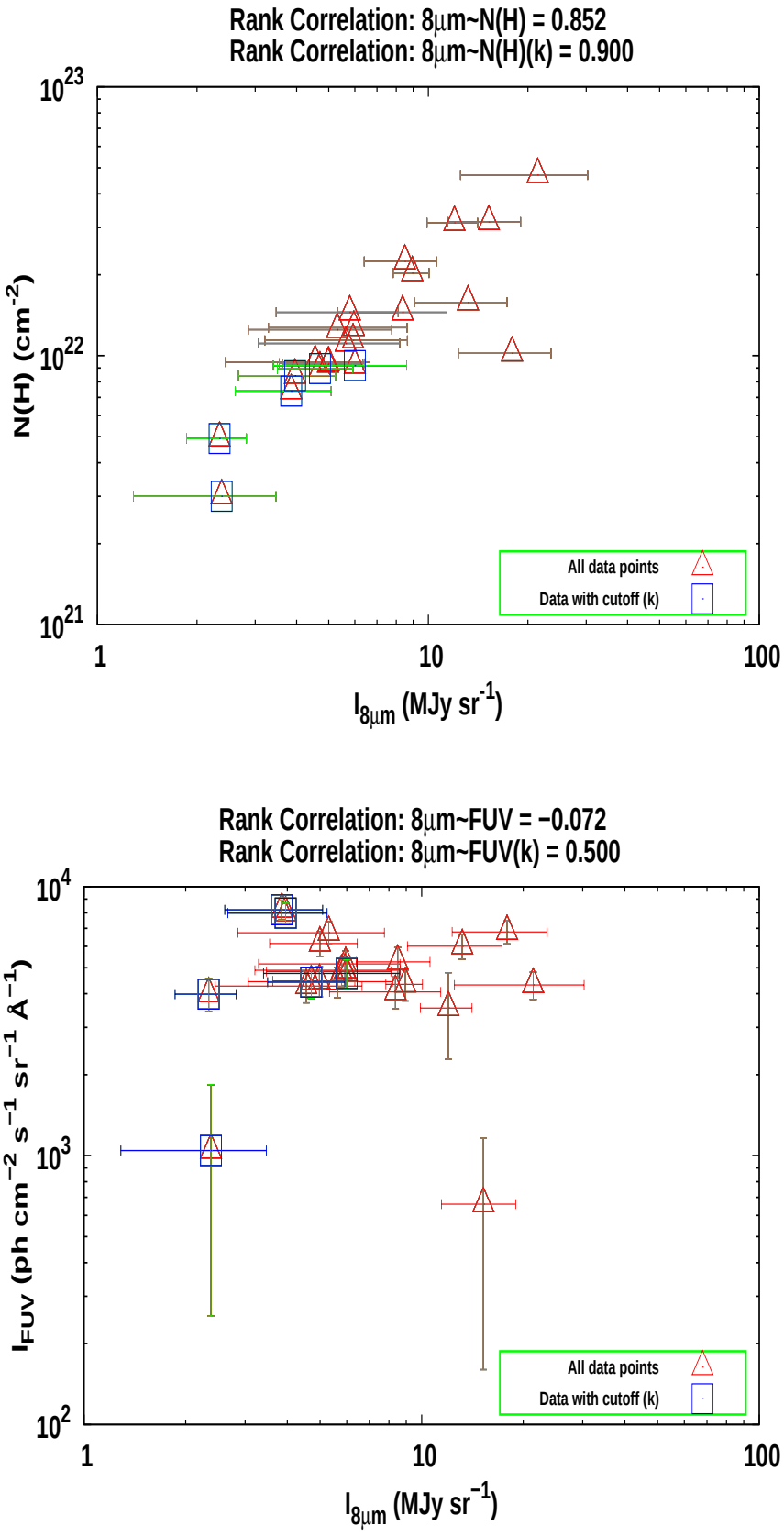

Figure 2.2: Correlations plotted for 8 μm vs. N(H) and FUV intensity at low latitude. Here, k means a cutoff for N(H) at 9×10^{21} cm^{-2}.

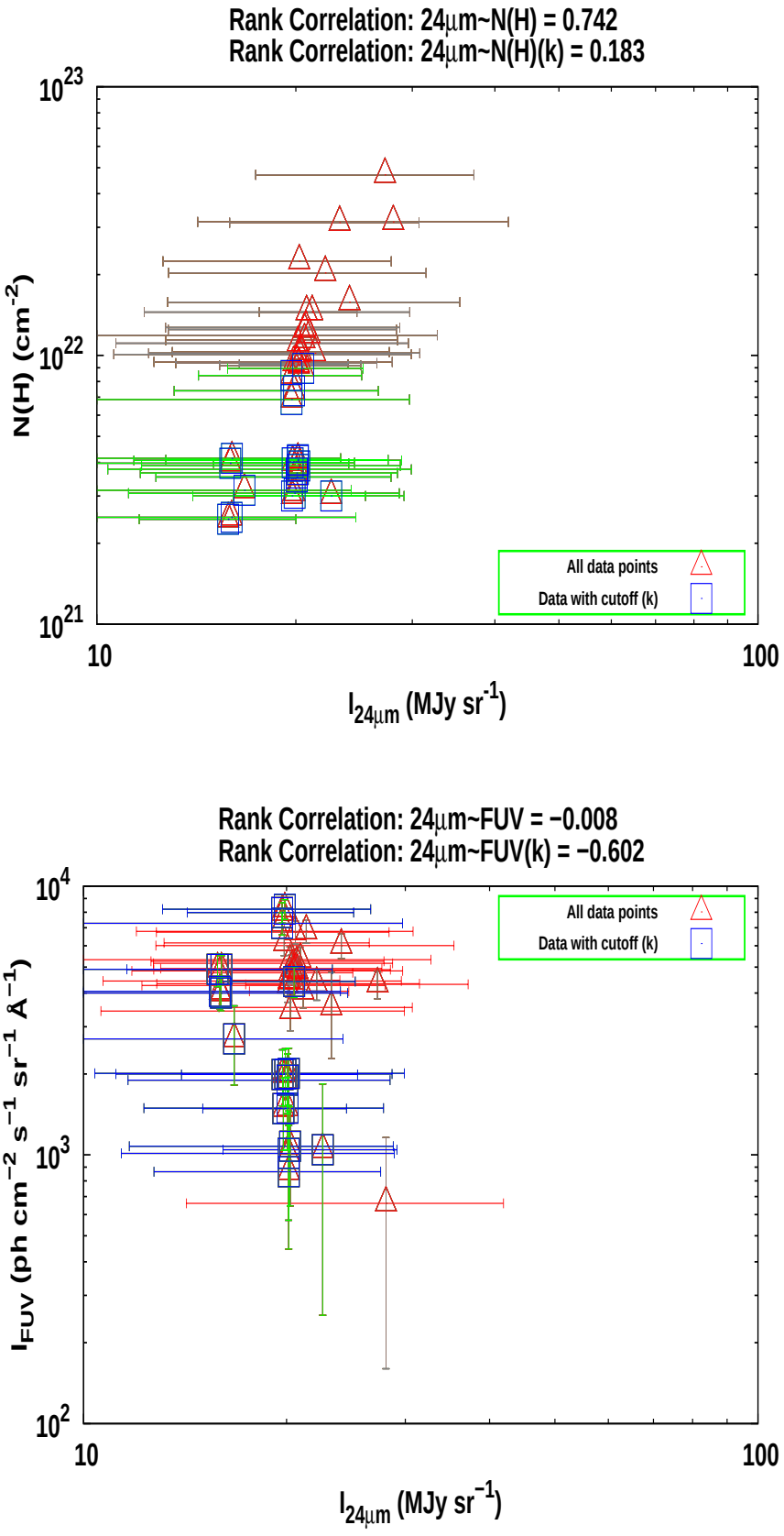

Figure 2.3: Correlations plotted for 24μm vs. N(H) and FUV intensity at low latitude. Here, k means a cutoff for N(H) at 9×10^{21} cm^{-2}.

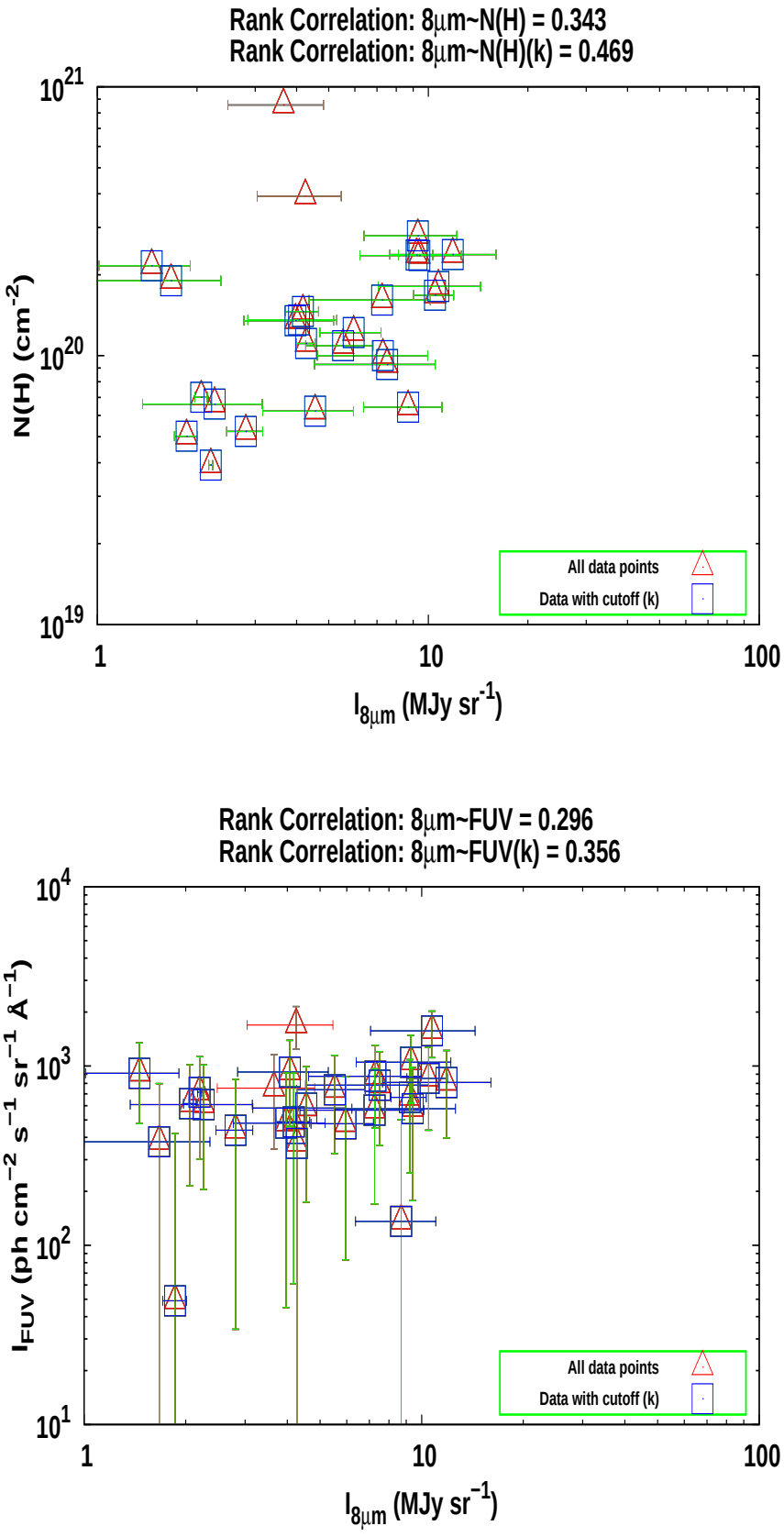

Figure 2.4: Correlations plotted for 8 μm vs. N(H) and FUV intensity at high latitude. Here, k means a cutoff for N(H) at 3×10^{20} cm^{-2}.

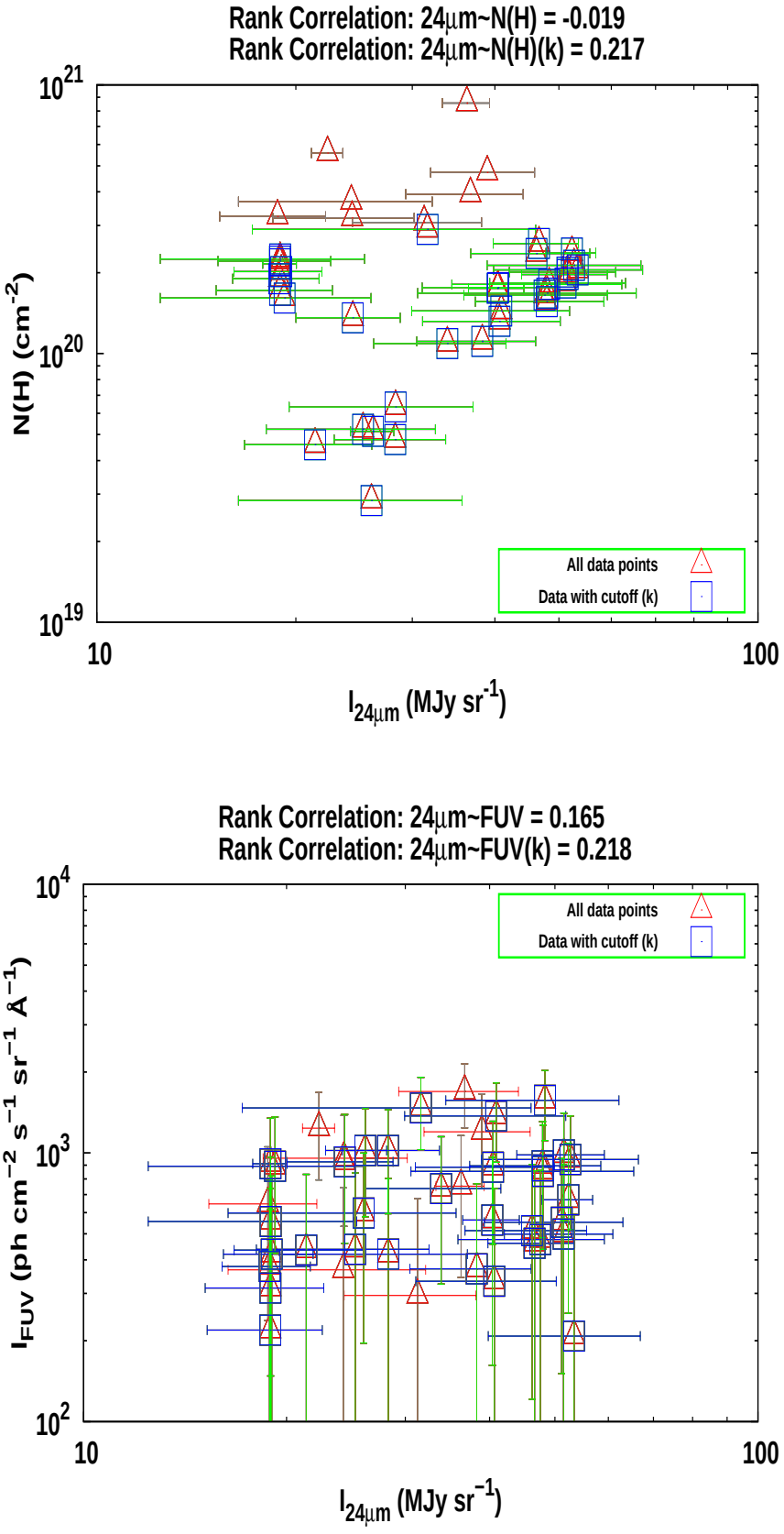

Figure 2.5: Correlations plotted for 24 μm vs. N(H) and FUV intensity at high latitude. Here, k means a cutoff for N(H) at 3×10^{20} cm^{-2}.

2.4 Discussion and Conclusions

We see from our low latitude correlation results presented in Table 2.1 that the 8 μm intensity is better correlated to the N(H) as compared to 24 μm intensity. Now, we know that N(H) is a direct measure of the intensity at 100 μm. Hence, this means that PAHs emitting around MIR 8 μm are associated with cold diffuse regions of the ISM which show emissions around FIR 100 μm [112–114]. The comparatively lower correlation between 24 μm and 100 μm is also expected because these are associated with grains in different environments, i.e. the 24 μm emission is from hot VSG populations [115, 116] while the 100 μm emission is from larger/colder grains. The p-values for most of the IR vs. FUV intensities in Table 2.1 are too high for the observed correlation values to be reliable. The only exception is the case of 24 μm vs. FUV (k) intensity, with cutoff on N(H), which shows a good negative correlation, i.e. as the FUV intensity increases, the IR emission decreases and vice versa. This could be because of absorption which reduces the FUV intensity in regions of high dust density. It is interesting to find that this negative correlation is seen in regions of low N(H) where no correlation is seen between the N(H) and 24 μm intensities (Table 2.1).

On the other hand, from the correlation coefficients at high latitude locations presented in Table 2.2, we do not get find any reliable p-values either for 8 μm or 24 μm data with the exception of only 8 μm vs. N(H) (k), with cutoff on N(H), which shows a much lower correlation value as compared to lower latitudes. This indicates that as we move to higher latitudes, the correlations go on getting lower probably due to decreasing abundance of interstellar PAHs and VSGs which supports the presence of interstellar dust in the lower latitude locations. At high latitudes, we expect much weaker FUV radiation since a significantly lower population of young stars is expected as compared to lower latitudes. The FUV radiation observed at high latitudes may be the scattered light from far-off dust [113, 117].

Murthy (2014, 2016) [75, 106] have observed and modelled, using Monte Carlo models with multiple scattering, the FUV and near-UV all-sky *GALEX* data in our Galaxy and identified high latitude regions where there is an offset between the model predictions and the observed data. These are shown as red coloured patches in Figure 2.1 and they seem to coincide with regions that are not in the ecliptic plane, i.e. plane of the solar system where planetary dust contributes. We see this in NASA's Diffuse Infrared Background Experiment (DIRBE) maps as shown in Figure 2.6 [118]. The bright diagonal line is the

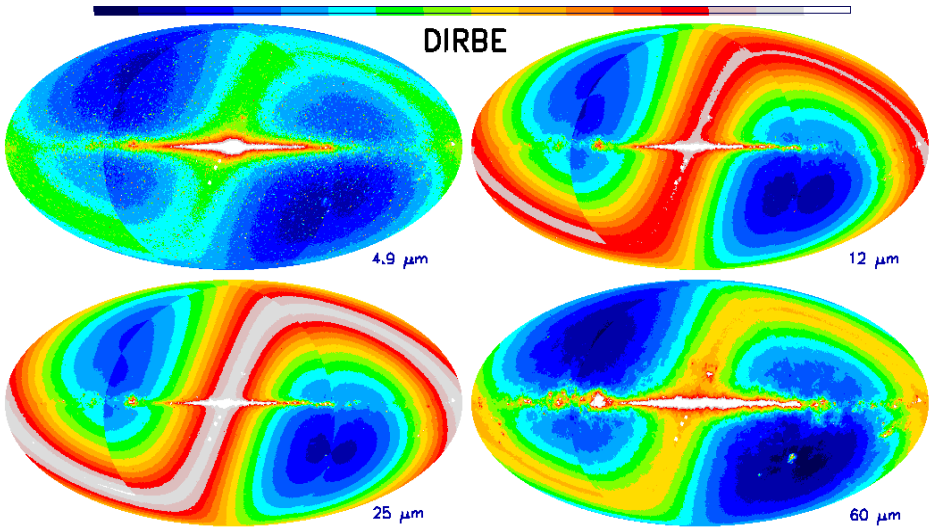

Figure 2.6: DIRBE maps [118] explaining our observed correlations.

ecliptic. The regions in the other two quadrants do not have contribution from the ecliptic plane and so they truly represent pure interstellar dust with some extragalactic contribution. Since some of our diffuse dust locations (Figure 2.1) fall into these regions of asymmetry, this might explain the low correlation values we are getting at high latitudes.

In conclusion, we find that both 8 μm and 24 μm emissions (Figures 2.2 and 2.3) have good positive correlations with N(H), with the 8μm correlation being comparatively better, while 24 μm has a good negative correlation with the FUV data at lower latitude locations. The PAH emission around 8 μm shows a better correlation with cold dust emissions and the VSG emission around 24 μm is from hot dust, i.e. both belong to different dust populations. The negative correlation shows that the FUV absorption is predominantly due to hot dust grains. This is also evident in the lack of correlation between the N(H) and 24 μm emission for locations where the FUV vs. 24 μm correlation is significant, i.e. with cutoff on N(H). The correlations are significantly better in low latitude locations as compared to high latitude locations (Figures 2.4 and 2.5) which indicates a decreasing abundance of interstellar PAHs and VSGs at high latitudes. Earlier studies [106] have not found any correlation among the FUV and 100 μm emission which can be attributed to two reasons: high latitude and VSG dominance; since we did find a good correlation between 24 μm intensity and N(H), i.e. emission at 100 μm (Table 2.1). The DIRBE maps (Figure 2.6) seem to indicate a remote origin for the observed FUV intensities at high galactic latitudes and hence support the claim for an extragalactic contribution at locations which are far from the ecliptic plane.